

SnO₂:F coated ferritic stainless steels for PEM fuel cell bipolar plates

Heli Wang*, John A. Turner

National Renewable Energy Laboratory, 1617 Cole Boulevard, Golden, CO 80401, USA

Received 2 February 2007; received in revised form 11 April 2007; accepted 12 April 2007

Available online 22 April 2007

Abstract

Ferrite stainless steels (AISI441, AISI444, and AISI446) were successfully coated with 0.6 μm thick SnO₂:F by low-pressure chemical vapor deposition and investigated in simulated PEMFC environments. The results showed that a SnO₂:F coating enhanced the corrosion resistance of the alloys in PEMFC environments, though the substrate steel has a significant influence on the behavior of the coating. ICP results from the testing solutions indicated that fresh AISI441 had the highest dissolution rates in both environments, and coating with SnO₂:F significantly reduced the dissolution. Coating AISI444 also improved the corrosion resistance. Coating AISI446 steel further improved the already excellent corrosion resistance of this alloy. For coated steels, both potentiostatic polarizations and ICP results showed that the PEMFC cathode environment is much more corrosive than the anode one. More dissolved metallic ions were detected in solutions for PEMFC cathode environment than those in PEMFC anode environment. Sn²⁺ was detected for the coated AISI441 and AISI444 steels but not for coated AISI446, indicating that the corrosion resistance of the substrate has a significant influence on the dissolution of the coating. After coating, the ICR values of the coated steels increased compared to those of the fresh steels. The SnO₂:F coating seems add an additional resistance to the native air-formed film on these stainless steels.

Published by Elsevier B.V.

Keywords: Bipolar plate; Stainless steel; Ferrite; Tin oxide; PEMFC

1. Introduction

Major challenges for the use of stainless steels as bipolar plates in a polymer electrolyte membrane fuel cell (PEMFC) include the corrosion resistance in the fuel cell anode and cathode environments and the interfacial contact resistance (ICR) [1]. Although previous investigations showed that stainless steels have a reasonably low contact resistance and good corrosion resistance in PEMFCs [2–8], the contact resistance with these bare stainless steels is still too high, resulting in reduced fuel cell performance. In terms of the corrosion resistance of the steels, it is clear that the lower the corrosion rate the better. Dissolution of thin plates can lead to breakthrough and fuel cell failure. Additionally, metallic ions coming from the corrosion may contaminate the membrane, significantly decreasing membrane conductivity and lowering the efficiency of the fuel cell.

Therefore, approaches to improve the stainless steel surface so as to have a lower contact resistance and better corrosion resistance are needed. Previously, the surface modification of ferritic AISI446 via thermal nitridation resulted in a modification of the native passive film of the alloy, significantly decreasing the ICR and improving the corrosion resistance in simulated PEMFC environments [9]. This approach may not be viable in all cases, which led us to investigate other possibilities. Our approach in looking for coatings is to identify base metals with high corrosion resistance and then apply a coating that is not only corrosion resistant but also provides low interfacial contact resistance. In this approach, the metal does not need to be pin-hole free since any exposure of the base metal will result in passivation. Previous work was conducted on applying conductive SnO₂ coatings onto metal substrates for the PEMFC bipolar plate, mostly as a protective coating on a porous substrate or as a catalyst [4,7]. In a previous paper, we reported on the results for a SnO₂:F coating on austenite stainless steels [10]. In this paper we will describe our work with this coating on ferritic stainless steels. Ferritic AISI446 showed much better corrosion resistance in the accel-

* Corresponding author. Tel.: +1 303 275 3858; fax: +1 303 275 2905.
E-mail address: heli.wang@nrel.gov (H. Wang).

erated PEMFC environments than 316L [6], while AISI441 and AISI444 are low cost alloys due to their low alloying elements content [6].

2. Experimental

2.1. Materials and electrochemistry

Stainless steels plates of AISI441, AISI444, and AISI446 were provided by J&L Specialty Steel, Inc., now part of Allegheny Ludlum. The chemical compositions have been given elsewhere [6]. Alloy plates were cut into samples of 2.54 cm × 1.25 cm (1.0 in. × 0.5 in.). The samples were treated with #600 grit SiC abrasive paper, rinsed with acetone, and dried with nitrogen gas.

The fluorine-doped SnO₂ (SnO₂:F) coating was prepared via a low-pressure chemical vapor deposition (LPCVD) system [11], using ultrahigh-purity (UHP) tetramethyltin (TMT, Morton International) and bromotrifluoromethane (CBrF₃) as tin and fluorine precursors, respectively, and UHP-grade oxygen as the oxidizer. The reaction chamber pressure for this study was kept at 50 Torr during deposition and the deposition temperature was 550 °C. The film thickness and the sheet resistance were measured by depositing SnO₂:F films on a glass substrate and using a stylus profilometer (Dektak3) for the thickness measurement and a Tencor M-gauge for the resistivity. Under the stated reaction conditions, a 0.6 μm thickness of SnO₂:F film was formed with a sheet resistance of 8 Ω/sq (or a resistivity of 5 Ω cm). No attempt was made to form pin-hole free films.

The electrode preparation for electrochemical measurements has been described previously [5,6,8]. All electrochemical experiments were conducted at 70 °C in 1 M H₂SO₄ + 2 ppm F⁻ solution and the solution was bubbled thoroughly with either hydrogen gas (for simulating a PEMFC anode environment) or pressured air (for simulating a PEMFC cathode environment) prior to and during the electrochemical measurements. The setup for the electrochemical measurements has been described in detail [5,6,10]. These conditions are for accelerated laboratory tests and effectively simulate the direct contact between the bipolar plate and the membrane.

2.2. Interfacial contact resistance

All ICR measurements were carried out at room temperature. The method for conducting ICR measurements has been previously described [5]. Briefly, two pieces of conductive carbon paper were sandwiched between the stainless steel sample and two copper plates. A current of 1.000 A was provided via the two copper plates and the total voltage drop was registered. Gradually increasing the compaction force allowed us to calculate the dependence of the total resistance on the compaction force. The ICR value of the carbon paper/copper plate interface ($R_{C/Cu}$) was compensated for with a calibration, so in this paper we give only the ICR values for the carbon paper/stainless steel interface. Both fresh and SnO₂:F coated steels were investigated. Fresh steel samples were used to baseline the carbon paper/stainless steel interface resistance ($R_{C/SS}$). For the SnO₂:F coated steel samples, the interfacial contact resistance due to

the uncoated backside was deducted using the previous measurements with the fresh steel samples, so only the ICR of the carbon paper/SnO₂:F coated steel interface ($R_{C/TO}$) was used in this paper.

2.3. Characterization with XRD, AES, and ICP

X-ray diffraction (XRD), was accomplished with a four-circle Scintag X-1 diffractometer (ThermoLab) with a Cu Kα anode source, and was used to investigate the structure of the SnO₂:F on the coated steel samples. A glancing angle XRD technique was used to investigate the structures of the bulk and surface layers. The noise-to-signal ratio was reduced by using a slow scanning speed of 0.02 °/step and a preset time of 3 s/step for all of the measurements.

The SnO₂:F coating's composition and the depth profile was determined by Auger electron spectroscopy (AES) analysis and was carried out using a Phi670 Auger Nanoprobe with a chamber base pressure of 4.0×10^{-8} Pa (3×10^{-10} Torr). The depth profiles were obtained by sputtering with 3 keV argon ions with a current density of around 1 μA/mm², and a system pressure in the chamber of approximately 6.67×10^{-6} Pa (5×10^{-8} Torr). Based on the previous measurements, a reasonable estimate of the sputtering rate was approximately 35 nm/min.

Test solutions (80–100 ml) were collected after 7.5 h of potentiostatic polarization with both coated and uncoated steels, purged either with air or hydrogen gas. An inductive coupled plasma (ICP) spectrometer was used to quantify the metallic Fe, Cr, Ni, and Sn ions dissolved in the collected solutions. The ICP system was a Varian Liberty 150 ICP Emission Spectrometer controlled by a PC. A standard solution, containing 100 ppm of each of the metal ions in 1 M H₂SO₄, was purchased from Inorganic Ventures, Inc. The estimated relative uncertainty for ICP analysis, mainly due to variability in the plasma, pump rate, and nebulizer efficiency, is 5% [12].

3. Results and discussion

3.1. XRD and AES characterization

Examples of the typical glancing angle XRD patterns for the SnO₂:F coated AISI446 stainless steel are shown in Fig. 1. At a glancing angle of 5°, both the ferrite structure of the steel and the coated SnO₂:F can be seen, corresponding to sampling a relatively deeper part of the surface. With a decreasing glancing angle, both the ferrite and the SnO₂:F peaks decrease, and at glancing angle of 1°, the ferrite peaks are negligible. On the other hand, all of the SnO₂:F peaks at a 1° glancing angle are still at a reasonable intensity, suggesting that the investigated area is totally composed of the SnO₂:F coating. Decreasing the angle further eliminates all of the signals. XRD patterns suggest that the SnO₂:F coating is in the μm scale, in agreement with the profilometer measurement. The XRD patterns at lower glancing angles for coated AISI446 are similar to those of the coated 349TM [10], as might be expected for the same surface coating.

Fig. 2a shows the AES depth profile of the SnO₂:F coated AISI446 stainless steel. At the start, only Sn and O are observed

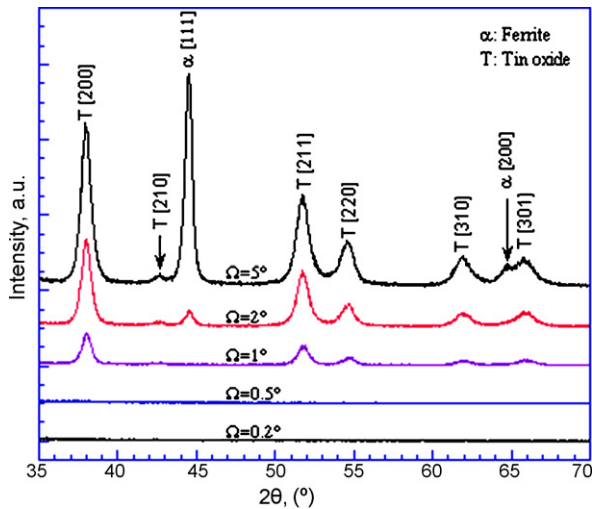


Fig. 1. Glancing angle X-ray diffraction patterns for AISI446 coated with $\text{SnO}_2\text{:F}$. Corresponding grazing angles (Ω) are marked.

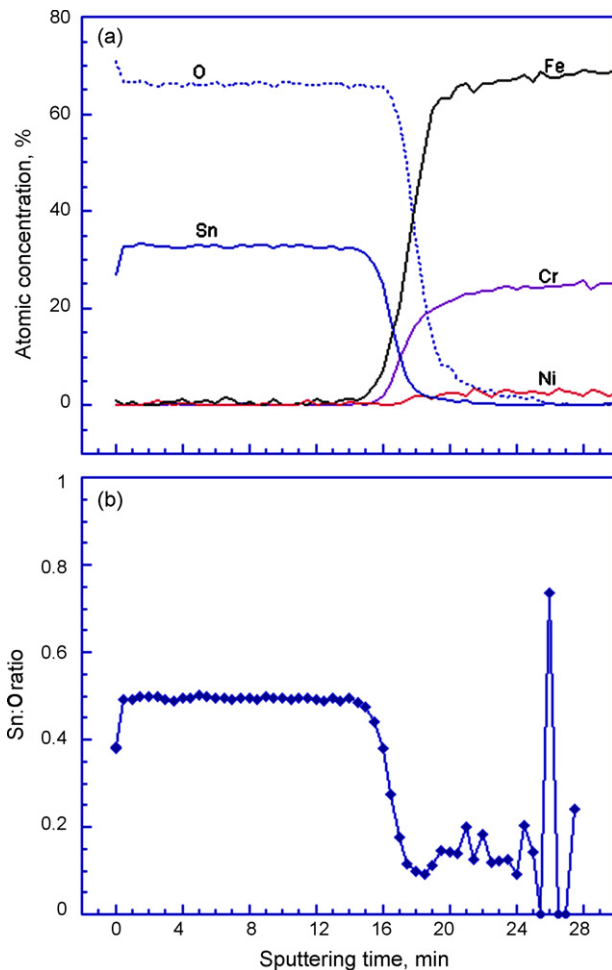


Fig. 2. AES depth profile for $\text{SnO}_2\text{:F}$ coated AISI446 steel (a); and the Sn:O ratio of the surface coating (b).

while the main steel compositional elements appear at longer sputtering times. This is very similar to results for $\text{SnO}_2\text{:F}$ coated 349TM steel [10], except for the difference in the substrate steel composition. Fig. 2b shows the Sn:O ratio against the sputtering

time; it also gives the general chemical composition of the SnO_2 coating. Because F is added only as a dopant, its concentration is insufficient to change the composition of the coating. Again, using the half value of the Sn:O ratio as the boundary of the $\text{SnO}_2\text{:F}$ and substrate steel, it took 17.0 min to sputter off the oxide coating. Assuming a sputtering rate of 35 nm/min, the coating thickness then is 0.60 μm , agreeing with the estimated value of 0.6 μm according to the deposition conditions as well as the XRD patterns.

3.2. Dynamic polarization of $\text{SnO}_2\text{:F}$ coated stainless steels

Fig. 3 shows the anodic polarization curves of $\text{SnO}_2\text{:F}$ coated stainless steels in 1 M $\text{H}_2\text{SO}_4 + 2 \text{ ppm } \text{F}^-$ at 70 °C purged with hydrogen gas. The PEMFCs anode operation potential of around -0.1 V is marked in the figure. The $\text{SnO}_2\text{:F}$ coating shows a behavior similar to the bare substrate for the AISI441 and AISI444 steels. It actually lowers the critical passivating current (Fig. 3a) for AISI441 and the passivation current (the lowest current to maintain passivation) for AISI444 (Fig. 3b) as compared to those of the fresh (bare) samples [6]. We noticed that -0.1 V is in the passive region for both coated steels and currents for coated AISI441 and AISI444 at this potential are lower than those for fresh steels, indicating the corrosion protection of the coating. For AISI441 and AISI444, Fig. 3a and b suggest that the difference in the polarization curves between coated steel and uncoated steel is not very significant. This could be related to the high passivating current for both steels in the environment. After experiencing the heavy surface dissolution, the dynamic behavior of the coated steels should be similar to the uncoated steels. The possible instability of SnO_2 at -0.1 V was noted also in the previous paper [10]. $\text{SnO}_2\text{:F}$ coated AISI446 shows a significantly different behavior from that of the fresh steel, Fig. 3c. The open circuit potential (OCP) of the coated AISI446 shifts anodically to *ca.* 0.09 V as compared with *ca.* -0.20 V for fresh AISI446 under the same conditions. Therefore, the anode potential in PEMFC application is located in the cathodic range of the polarization curve, indicating that a cathodic current (though likely very low) would be expected if the coated steel is polarized at this potential. Moreover, the current density for coated AISI446 throughout the whole polarization region is significantly reduced by over 1 order of magnitude. Both results for the $\text{SnO}_2\text{:F}$ coating on AISI446 are beneficial for its application as a PEMFC bipolar material. For comparison purposes, the dynamic polarization curves for all $\text{SnO}_2\text{:F}$ coated steels are shown in Fig. 3d. We see that the current density at -0.1 V is rather high for the $\text{SnO}_2\text{:F}$ coated AISI441 ($\sim 200 \mu\text{A}/\text{cm}^2$) and the AISI444 ($\sim 50 \mu\text{A}/\text{cm}^2$) steels, suggesting that these coated alloys would experience high current if operated at this potential. In comparison, the current at -0.1 V for the coated AISI446 is $\sim -0.4 \mu\text{A}/\text{cm}^2$.

In the PEMFC cathode environment, the $\text{SnO}_2\text{:F}$ coated AISI441 again shows a behavior similar to that of fresh AISI441 steel, Fig. 4a, but with a reduction in the critical passivating current. A current around $45 \mu\text{A}/\text{cm}^2$ is seen at 0.6 V. Combined with Fig. 3a, $\text{SnO}_2\text{:F}$ coated AISI441 under such conditions seems unsuitable for application as a PEMFC bipolar plate mate-

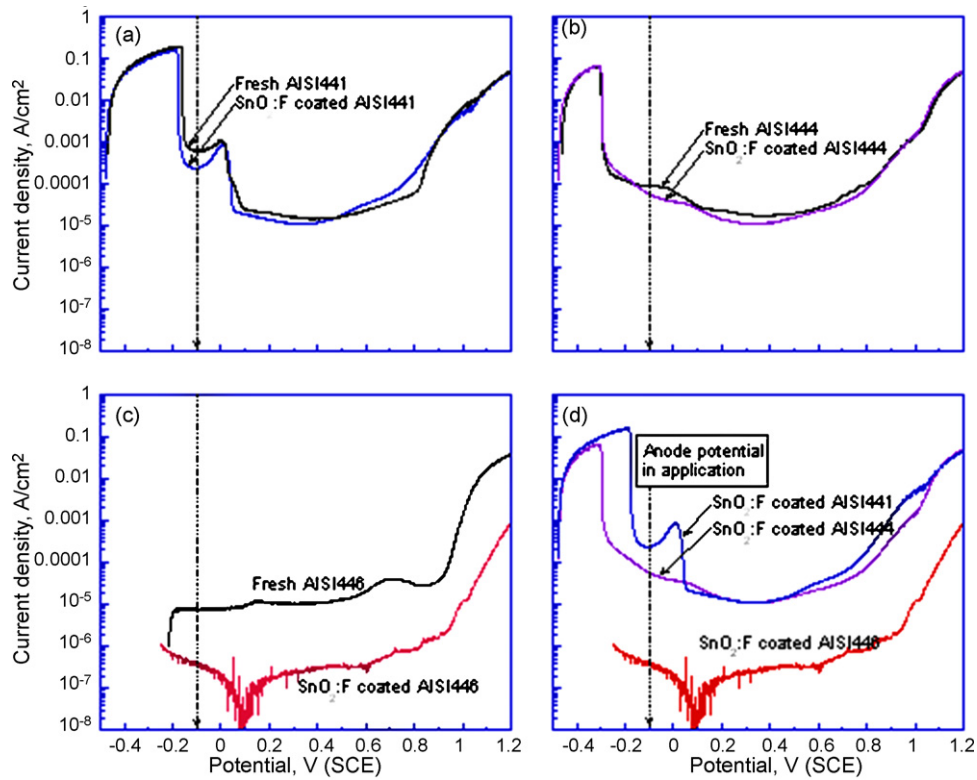


Fig. 3. Anodic behavior of fresh and $\text{SnO}_2\text{:F}$ coated ferrite stainless steels in $1\text{ M H}_2\text{SO}_4 + 2\text{ ppm F}^-$ at $70\text{ }^\circ\text{C}$ purged with H_2 . The anode potential in PEMFCs application is marked. (a) Fresh and $\text{SnO}_2\text{:F}$ coated AISI441; (b) fresh and $\text{SnO}_2\text{:F}$ coated AISI444; (c) fresh and $\text{SnO}_2\text{:F}$ coated AISI446; (d) $\text{SnO}_2\text{:F}$ coated steels.

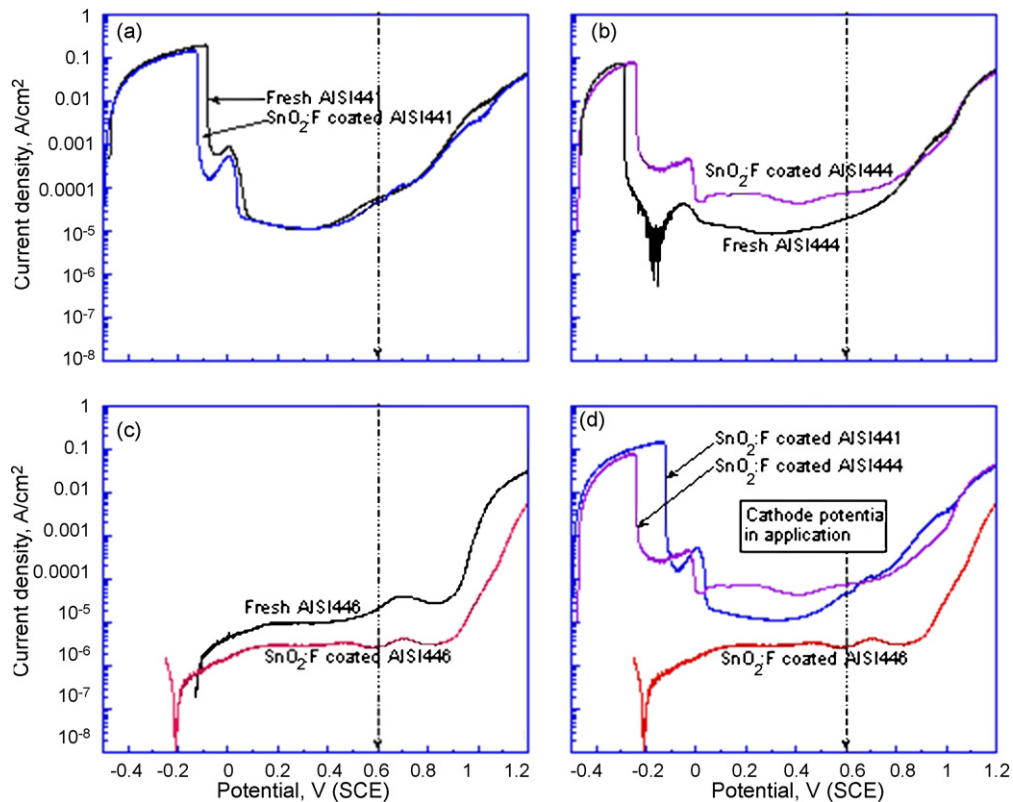


Fig. 4. Anodic behavior of fresh and $\text{SnO}_2\text{:F}$ coated ferrite stainless steels in $1\text{ M H}_2\text{SO}_4 + 2\text{ ppm F}^-$ at $70\text{ }^\circ\text{C}$ purged with air. The cathode potential in PEMFCs application is marked. (a) Fresh and $\text{SnO}_2\text{:F}$ coated AISI441; (b) fresh and $\text{SnO}_2\text{:F}$ coated AISI444; (c) fresh and $\text{SnO}_2\text{:F}$ coated AISI446; (d) $\text{SnO}_2\text{:F}$ coated ferrite stainless steels.

rial. Fresh AISI444 has a current density of *ca.* $20 \mu\text{A}/\text{cm}^2$ at 0.6 V in air-purged solution, while the $\text{SnO}_2:\text{F}$ coated AISI444 shows a current jump, with a value of *ca.* $75 \mu\text{A}/\text{cm}^2$ at this potential (Fig. 4b). At this time, this current increase is not understood. The current for the $\text{SnO}_2:\text{F}$ coated AISI446, is generally lower compared to the uncoated one (Fig. 4c). The current density at 0.6 V is *ca.* $2.7 \mu\text{A}/\text{cm}^2$ with the coated steel as compared with *ca.* $20 \mu\text{A}/\text{cm}^2$ for the fresh steel sample. Moreover, the OCP with coated steel shifts in the cathodic direction to *ca.* -0.2 V , as compared to *ca.* -0.1 V with uncoated steel. When compared with Fig. 3, we see that $\text{SnO}_2:\text{F}$ coated AISI446 is the best of this group in the simulated PEMFC environment. Again, this is likely related to the composition of the substrate steel.

3.3. Potentiostatic polarization of $\text{SnO}_2:\text{F}$ coated stainless steels

To investigate the stability of the $\text{SnO}_2:\text{F}$ coating in a simulated PEMFC anode environment, we carried out potentiostatic polarization measurements for the coated steels at -0.1 V in a solution purged with hydrogen gas; the current \sim time behavior is shown in Fig. 5. As soon as the potential is applied, there is a sharp current decrease for coated AISI441 and AISI444 (Fig. 5 inset), with the $\text{SnO}_2:\text{F}$ coated AISI446 showing the sharpest current drop. $\text{SnO}_2:\text{F}$ coated AISI441 takes *ca.* 30 min before stabilizing at *ca.* $10 \mu\text{A}/\text{cm}^2$ followed by a slow but steady current increase after *ca.* 70 min polarization. The current increases to *ca.* $35 \mu\text{A}/\text{cm}^2$ at the end of the experiment. For coated AISI444, there is an anodic \sim cathodic current transition at *ca.* 50 min. A similar transition was reported previously [5]. The current crosses back to anodic again at *ca.* 210 min of polarization, followed by a slight current increase. The current reaches *ca.* $7.5 \mu\text{A}/\text{cm}^2$ at the end of the experiment. As for the $\text{SnO}_2:\text{F}$ coated AISI446, except for the current drop in the beginning of the test, the current is cathodic in the whole polarization period. A cathodic current indicates that the material is

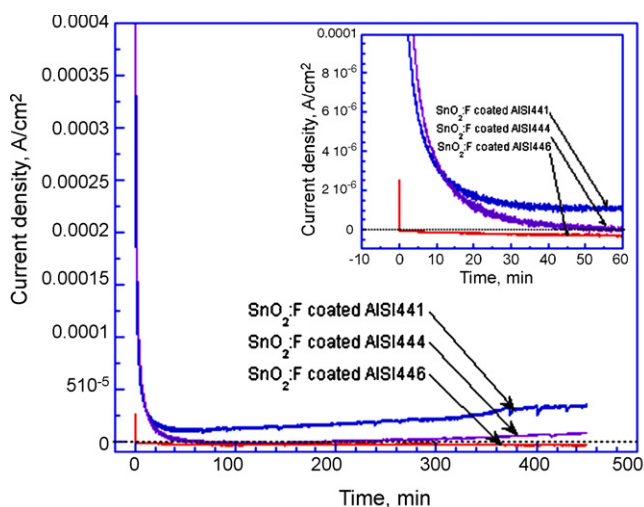


Fig. 5. Transient currents of $\text{SnO}_2:\text{F}$ coated ferrite stainless steels at -0.1 V in $1 \text{ M H}_2\text{SO}_4 + 2 \text{ ppm F}^-$ at 70°C purged with hydrogen gas (anode environment). Insert shows the transient currents in the first hour of testing.

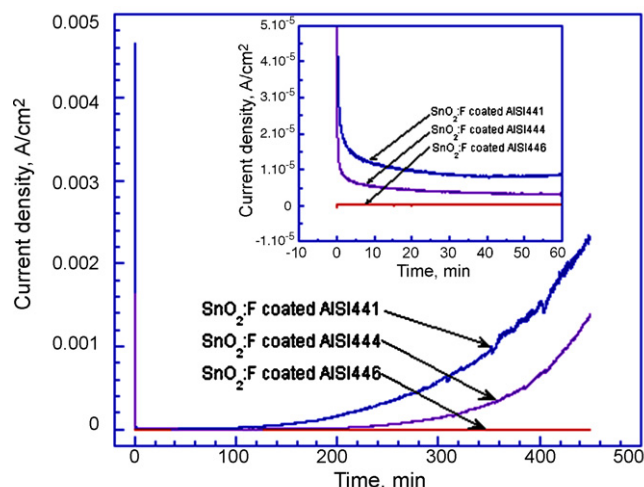


Fig. 6. Transient currents of $\text{SnO}_2:\text{F}$ coated ferrite stainless steels at 0.6 V in $1 \text{ M H}_2\text{SO}_4 + 2 \text{ ppm F}^-$ at 70°C purged with pressured air (cathode environment). Insert shows the transient currents in the first hour of testing.

cathodically protected and anodic dissolution (corrosion) is significantly eliminated, i.e., at the lowest possible rate. It should be mentioned that the reduction of Sn^{2+} from SnO_2 is also thermodynamically possible under these conditions. The current for the coated AISI446 is very stable, at -1 to $-3.5 \mu\text{A}/\text{cm}^2$ (Fig. 5). Such behavior was seen with thermally nitrated Ni-50Cr alloy and AISI446 steel in the same environment [9,13,14]. The potentiostatic polarization illustrates the superior performance of $\text{SnO}_2:\text{F}$ coated AISI446 in the PEMFC anode environment and its possible suitability as a coating for this bipolar plate material.

The cathode side in the PEMFC is oxygen reduction and the environment is oxidizing. Potentiostatic measurements were carried out at 0.6 V in a solution purged with air and the typical current \sim time behavior is shown in Fig. 6. The inset of Fig. 6 shows the current decay during the first hour of polarization. As soon as the potential is applied, the currents decay very fast for coated AISI441 and AISI444, even faster than those in the PEMFC anode environment, while the $\text{SnO}_2:\text{F}$ coated AISI446 has almost no current decay. $\text{SnO}_2:\text{F}$ coated AISI441 experiences a stable current of *ca.* $8\text{--}9 \mu\text{A}/\text{cm}^2$ after *ca.* 30 min polarization, and then after *ca.* 90 min polarization there is a steady current increase. This is very similar to its behavior in the PEMFC anode environment (Fig. 5). However, the current increase for the coated AISI441 in the PEMFC cathode environment is much faster than that in the anode environment. The current reaches *ca.* $2.30 \text{ mA}/\text{cm}^2$ at the end of 450 min polarization. Similar behavior is noted for $\text{SnO}_2:\text{F}$ coated AISI444 steel, where a stable lower current of *ca.* $3.5 \mu\text{A}/\text{cm}^2$ is obtained after *ca.* 30 min. Moreover, the current shows greater stability for the coated AISI444 than for the coated AISI441, with a current increase after *ca.* 180 min. After 450 min polarization, the current for coated AISI444 reaches *ca.* $1.40 \text{ mA}/\text{cm}^2$, which is lower than that for coated AISI441. In contrast, only a small current spike is seen with the $\text{SnO}_2:\text{F}$ coated AISI446 at the beginning of polarization (Fig. 6 inset). The current with the coated AISI446 is extremely stable for the whole test period and

is within the range of 0.2 to $1 \mu\text{A}/\text{cm}^2$. This is in agreement with the dynamic polarization results (Fig. 4) in which 0.6 V is in the middle of the passivation region for coated AISI446 and very low current is obtained at this potential. To check the possible influence of the oxygen reduction reaction under these conditions, we applied 0.6 V to a Pt plate (an excellent oxygen reduction reaction catalyst) at identical conditions. A continuously decaying anodic current was registered and it reached *ca.* $1.2 \mu\text{A}/\text{cm}^2$ after ~ 10 min. This blank test indicates that the oxygen reduction does not play a significant role in the observed sample current when polarized at 0.6 V in the air-purged solution.

The above electrochemical results again show the importance of the composition of the underlying alloy on the performance of the $\text{SnO}_2:\text{F}$ coated steels, with the coated AISI446 giving the best behavior in the simulated PEMFC environments. $\text{SnO}_2:\text{F}$ coated AISI444 shows improved behavior in a PEMFC anode environment, while somehow a high anodic current is still seen in the PEMFC cathode environment. A much higher anodic current is also obtained with the coated AISI441 in the PEMFC cathode environment than in anode environment. This substrate dependency is mostly due to the porous nature of the coating. The polarization results suggest that $\text{SnO}_2:\text{F}$ coating is more protective for AISI441 and AISI444 in the anode environment than the cathode environment. One would expect a lower anodic current for steels in the PEMFC cathode environment than in PEMFC anode one and this is not the case for these samples. Clearly some additional work is needed to fully understand this result.

3.4. Interfacial contact resistance

The interfacial contact resistance (ICR) between the $\text{SnO}_2:\text{F}$ coated stainless steel samples and the carbon paper was investigated as a function of compaction force (Fig. 7). ICR values with uncoated steels are also shown for comparison. For the uncoated steels, AISI444 has the lowest ICR values in the whole compaction force range investigated, with AISI441 being slightly higher and AISI446 showing the highest ICR values among the three steels tested [6]. We see that the ICR values increased for the steels coated with $\text{SnO}_2:\text{F}$, which is a different result than that for austenite steels [10]. Again, the $\text{SnO}_2:\text{F}$ coated AISI444 shows the lowest ICR values among the three coated steels; the $\text{SnO}_2:\text{F}$ coated AISI441 has slightly higher ICR values than those of the coated AISI444, and the $\text{SnO}_2:\text{F}$ coated AISI446

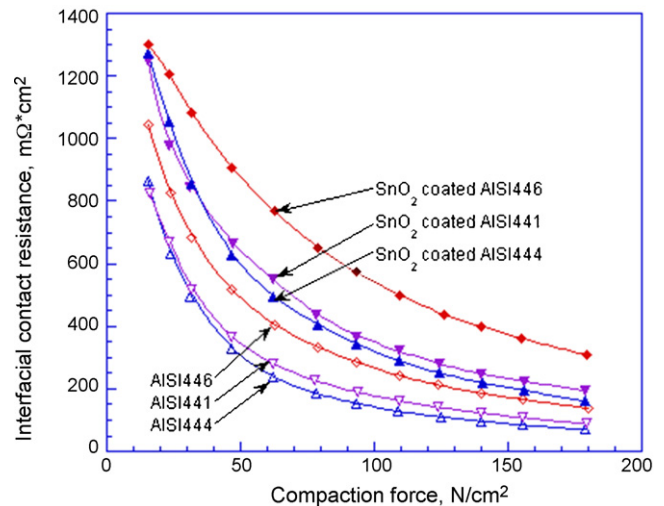


Fig. 7. Interfacial contact resistances for fresh and SnO_2 coated stainless steels and carbon paper at different compaction forces.

shows the highest ICR values among the three coated steels. The increase of the ICR values is not desirable since this will result in power losses for the application as a PEMFC bipolar plate. The behavior could be due to the accumulative effect of the $\text{SnO}_2:\text{F}$ coating on the native oxide layer. One way to improve the ICR could be by controlling the deposition processing and parameters such that the native surface oxide film on stainless steels is modified before or during the $\text{SnO}_2:\text{F}$ deposition process. We are currently investigating such an approach.

3.5. Dissolved metallic ions

The metal ions dissolved during 7.5 h of potentiostatic polarization with fresh and $\text{SnO}_2:\text{F}$ coated steels were analyzed by ICP and the results are shown in Table 1.

In all cases, Fe was found in the highest concentration. This is in agreement with our previous XPS investigation on the passive film where Fe was selectively dissolved and Cr was enriched at the surface [8,15], and to be expected based on the steel's composition. Fresh AISI441 showed the highest concentrations of dissolved Fe, Cr, and Ni, and it experienced higher dissolution in the PEMFC anode (hydrogen) environment than in the PEMFC cathode (air) environment. The heavy dissolution indicates that this bare alloy is not suitable for use as a bipolar plate [6]. When coated with $\text{SnO}_2:\text{F}$, there is a significant decrease in the dis-

Table 1

Fe, Cr, Ni, and Sn ion concentrations for bare and $\text{SnO}_2:\text{F}$ coated stainless steels after 7.5 h polarization in PEMFC environments (average of three samples)

Material	Ion content after 7.5 h in PEMFC anode (H_2) environment (ppm)				Ion content after 7.5 h in PEMFC cathode (air) environment (ppm)			
	Fe	Cr	Ni	Sn	Fe	Cr	Ni	Sn
AISI441	622.9	135.7	1.07	–	462.8	101.2	0.95	–
AISI444	141.5	37.86	0.30	–	328.3	67.97	0.94	–
AISI446	1.46	–	–	–	0.99	–	–	–
$\text{SnO}_2:\text{F}/\text{AISI441}$	24.15	4.51	–	2.42	330.3	73.53	0.60	22.76
$\text{SnO}_2:\text{F}/\text{AISI444}$	12.70	2.09	–	1.76	64.42	13.73	0.22	4.50
$\text{SnO}_2:\text{F}/\text{AISI446}$	1.24	–	–	–	0.98	–	–	–

solution rate. In the PEMFC anode environment, Fe ions for the coated AISI441 are reduced by a factor of 25, Cr ions are reduced by a factor of 30, and Ni ions are below the detectable level as compared to the bare steel. In the PEMFC cathode environment, the dissolved metallic ions with coated AISI441 are roughly reduced 30% compared to those with bare AISI441, which is still remarkable. The reduction of metal ions in the test solution from the coated sample as compared to the bare steel in the simulated PEMFC anode environment is remarkable. On the other hand, for the coated AISI441, 2.42 ppm and 22.76 ppm of Sn are detected in the PEMFC anode environment and cathode environment, respectively. It is interesting that we found a much higher Sn dissolution in the PEMFC cathode environment than in the anode environment. This could be related to the corrosion resistance of the substrate material in the environment and the coating quality (pin-holes), as well as the stability of the coating material. Since the AISI446 was coated in identical conditions and the coated steel has no detectable Sn ion during the tests (Table 1), the substrate material obviously plays a major role in the dissolution of the coating. Anyway, this data illustrates the protection of the SnO₂:F coating on AISI441, and is in excellent agreement with the polarization curves where coated AISI441 experienced a much higher anodic current in the PEMFC cathode environment than that in the anode one (Figs. 5 and 6). ICP data also point out that one could not use the dynamic polarization curve to predict the anodic dissolution rate. In our case, although the polarization curves of coated and uncoated AISI441 are similar, the metal ion concentrations are really rather different. On the other hand, the potentiostatic polarization experiments provide a better estimate for comparison. For bare AISI444 steel, the metal dissolution rate is lower than AISI441, and the dissolved metallic ions in the simulated cathode environment are about double those in the PEMFC anode environment. With the SnO₂:F coating in the PEMFC cathode environment, there are five times fewer dissolved Fe, Cr, and Ni ions than in the uncoated steel. Significant improvement is also seen in the PEMFC anode environment for the coated AISI444 where dissolved Fe ions are reduced by more than 11 times and Cr is reduced over 18 times compared to the uncoated sample. Sn ions were detected with 1.76 ppm in the PEMFC anode environment and 4.50 ppm in PEMFC cathode environment. This is much less than in the coated AISI441, due to a higher corrosion resistance of the substrate AISI444 steel in PEMFC environments. Again, these data confirm the corrosion protection of the SnO₂:F coating on the steels and are in good agreement with the polarization curves (Figs. 5 and 6). Note that there are more dissolved metallic ions for coated AISI444 in the PEMFC cathode (air) environment than in the anode (hydrogen) one, regardless of the coating. This is the same for coated AISI441. Since the PEMFC anode environment is reductive and the cathode one is oxidative, the passive film of stainless steel should be more stable in the later condition. However, the experimental data, both the polarization curves and the ICP analysis indicate that the coating is more protective in the PEMFC anode environment than in the cathode environment. This could be related to the reduction of Sn²⁺ from SnO₂ in the later environment. Additional work is needed to understand this behavior.

Note that, in contrast to the other alloys, the bare AISI441 alloy showed a much higher dissolution rate in the hydrogen environment than in the air environment. The stability and the ability to maintain a passive film in a particular fuel cell environment clearly depend on the alloy composition. Both the AISI441 and the AISI444 have about the same chromium percentage, and neither have much nickel. The major difference is the small amount of Mo (~2%) in the AISI444, again pointing towards the need to understand the impact of minor constituents on the performance of the alloy in a bipolar plate application.

Previously, we determined that AISI446 was a good candidate steel for PEMFC environments with a low corrosion rate [6]. The dissolved metallic ions in both PEMFC environments give only ppm levels of Fe, confirming the low dissolution rate of the alloy and its high corrosion resistance in the PEMFC environments. Since AISI446 is already excellent in terms of its corrosion resistance in PEMFC environments, the possible improvement by means of a coating is rather limited. Table 1 reveals such performance and indicates that the SnO₂:F coating is only somewhat beneficial to AISI446 in terms of improving its corrosion resistance. Moreover, Sn ions are below the detectable level due to the superior corrosion resistance of the bare AISI446 in the environments. Nevertheless, Table 1 confirms that AISI446, with or without SnO₂:F coating, has the lowest dissolution rate of these samples in these environments. The primary attempt to coat AISI444 with SnO₂:F is promising in terms of corrosion resistance and confirms the feasibility of the method, though some further work is needed to improve the corrosion resistance before that alloy/coating combination could be considered for PEMFC environments.

4. Conclusions

We compared the performance of SnO₂:F coated and uncoated ferrite stainless steels in 1 M H₂SO₄ + 2 ppm F⁻ at 70 °C purged either with hydrogen gas or pressured air, and determined that the substrate steel has a significant influence on the polarization behavior of the coated steel. This could be related to the porous nature of the coating.

The ICR results were disappointing in that the ICR values increased significantly with the SnO₂:F coating. Clearly the SnO₂:F coating seems to add an additional resistance to the air-formed film on these stainless steels. So, from the ICR point of view, the air-formed film of stainless steels should either be modified before the deposition of the SnO₂:F coating, or the coating parameters must be varied in order to have a lower ICR resistance in the final coated film.

In the PEMFC anode environment, anodic current for SnO₂:F coated AISI441 reached ~35 μA/cm² at the end of the 7.5 h test. In the PEMFC cathode environment, the current for coated AISI441 reached ~2.30 mA/cm² at the end of the test. For coated AISI444 in a PEMFC anode environment, the current after 30 min polarization was reasonably stable at -2 to 8 μA/cm². In the PEMFC cathode environment, the anodic current stabilized at ~3.5 μA/cm² until *ca.* 180 min when an increase occurred. It reached ~1.40 mA/cm² for the coated AISI444 at the end of the test. As for SnO₂:F coated AISI446 in the PEMFC anode

environment, the current was cathodic for the entire polarization period, an indication that the material is cathodically protected and the anodic dissolution is at the lowest possible rate. The current stayed in the -1 to $-3.5 \mu\text{A}/\text{cm}^2$ range, and was extremely stable. In a PEMFC cathode environment, the coated AISI446 is also very stable, with a current of 0.2 to $1.0 \mu\text{A}/\text{cm}^2$ for the entire polarization period. In terms of corrosion resistance in PEMFC environments, coated AISI446 seems the best for bipolar plate application among the coated steels.

The ICP results for the dissolved metal ions agreed well with the potentiostatic polarization experiments. More dissolved metallic ions were detected in solutions for the PEMFC cathode environment than for the PEMFC anode environment. Sn^{2+} was detected for the coated AISI441 and AISI444 steels, but not for coated AISI446, indicating that the corrosion resistance of the substrate has a significant influence on the dissolution of the coating. The $\text{SnO}_2\text{:F}$ coating enhanced the corrosion resistance of all the alloys in the PEMFC environments, showing a greater enhancement for AISI441 and AISI444 than AISI446, although bare AISI446 already shows good corrosion resistance so the ability of the coating to improve its corrosion resistance is limited. In addition, the high anodic current and high dissolved metallic concentration for coated AISI441 suggest that this material is not suitable for the bipolar plate application. The attempt to apply this coating on AISI444 is promising, though further work is needed to improve its corrosion resistance in the PEMFC cathode environment.

Acknowledgements

The authors wish to thank Dr. Xiaonan Li for the $\text{SnO}_2\text{:F}$ deposition, and Dr. Glenn Teeter for assistance with the AES

measurements. Dr. Raghu Bhattacharya is acknowledged for assistance in ICP analysis. This work was supported by the Hydrogen, Fuel Cell and Infrastructure Technologies Program of the US Department of Energy.

References

- [1] B.C.H. Steele, A. Heinzl, *Nature* 414 (2001) 345.
- [2] R.C. Makkus, A.H.H. Janssen, F.A. de Bruijn, R.K.A.M. Mallant, *J. Power Sources* 86 (2000) 274.
- [3] D.P. Davies, P.L. Adcock, M. Turpin, S.J. Rowen, *J. Power Sources* 86 (2000) 237.
- [4] A.J. Appleby, S. Gamburgzev, US Patent 6,828,054 (2004).
- [5] H. Wang, M.A. Sweikart, J.A. Turner, *J. Power Sources* 115 (2003) 243.
- [6] H. Wang, J.A. Turner, *J. Power Sources* 128 (2004) 193.
- [7] B. May, D.R. Hodgson, US Patent 6,790,554 (2004).
- [8] H. Wang, G. Teeter, J.A. Turner, *J. Electrochem. Soc.* 152 (2005) B99.
- [9] H. Wang, M.P. Brady, K.L. More, H.M. Meyer III, J.A. Turner, *J. Power Sources* 138 (2004) 79.
- [10] H. Wang, J.A. Turner, X. Li, R. Bhattacharya, SnO_2 -coated austenite stainless steels for PEM fuel cell bipolar plates, *J. Power Sources*, in press.
- [11] X. Li, T.A. Gessert, T. Coutts, *Appl. Surf. Sci.* 223 (2004) 138–143.
- [12] R.N. Bhattacharya, A. Duda, D.S. Ginley, J.A. DeLuca, Z.F. Ren, C.A. Wang, J.H. Wang, *Physica C* 229 (1994) 145.
- [13] M.P. Brady, K. Weisbrod, I. Paulauskas, R.A. Buchanan, K.L. More, H. Wang, M. Wilson, F. Garzon, L.R. Walker, *Scripta Materialia* 50 (2004) 1017.
- [14] H. Wang, M.P. Brady, G. Teeter, J.A. Turner, *J. Power Sources* 138 (2004) 86.
- [15] H. Wang, J.A. Turner, On the passivation of 349TM, stainless steel in a simulated PEMFC cathode environment, in: T. Fuller, C. Bok, C. Lamy (Ed.), *ECS Transactions, Proton Exchange Membrane Fuel Cells V*, in honor of Supramaniam Srinivasan, vol. 1, No. 6, pp. 263–272.